Available online at www.sciencedirect.com
SCIENCE DIRECT®
ELSEVIER
Nuclear Instruments and Methods in Physics Research A 554 (2005) 300–305
NUCLEAR INSTRUMENTS & METHODS IN PHYSICS RESEARCH Section A
www.elsevier.com/locate/nima

1.3 kg bolometers to search for rare events

C. Arnaboldi[a], C. Brofferio[a], C. Bucci[b], P. Gorla[a,c], G. Pessina[a], S. Pirro[a,*]

[a]*Dipartimento di Fisica dell'Università di Milano-Bicocca and INFN, Sezione di Milano, I-20126 Milano, Italy*
[b]*INFN, Laboratori Nazionali del Gran Sasso, I-67010 Assergi (L'Aquila), Italy*
[c]*Laboratorio de Fisica Nuclear y Altas Energias, Universidàd de Zaragoza, 50009 Zaragoza, Spain*

Received 9 June 2005; received in revised form 27 July 2005; accepted 28 July 2005
Available online 18 August 2005

Abstract

Two TeO_2 crystal bolometers of 1.3 kg each, the largest single crystals ever operated with this technique, have been successfully realized and tested below 10 mK, in a dilution refrigerator located deep underground in the Gran Sasso National Laboratories. The calibration spectrum, obtained using an external ^{232}Th γ-ray source, shows an energy resolution of 3–4 keV FWHM from 0.5 to 2.6 MeV, for both detectors. In the α region, a 4.3 keV FWHM resolution has been observed on the 5407 keV peak due to the α decay of ^{210}Po, a natural contaminant of TeO_2 crystals.

PACS: 29.40.Vj; 29.30.Ev; 29.30.Kv; 07.20.Mc

Keywords: Cryogenic detectors; Double beta decay; Dark matter searches

1. Introduction

In the last years bolometers have become extremely powerful detectors in the search for rare events, like Double Beta Decay or Non-Baryonic Dark Matter, thanks to their excellent energy resolution. In this class of experiments the increase of the single module mass can be extremely helpful, for several reasons. First of all the Peak-to-Compton ratio for γ-rays interaction improves, allowing a better environmental background identification. Secondly, the surface-to-volume ratio becomes lower, thus determining a reduction of background per unit mass of the detector, since the radioactivity coming from surface impurities decreases. Finally, since a very large mass experiment requires always the use of an array of detectors, a larger single crystal mass corresponds to a lower number of read-out channels, with a consequent simplified setup.

The results reported here show that TeO_2 bolometers of 1.3 kg can reach performances similar to those obtained in the CUORICINO experiment with 0.8 kg detectors [1], while improv-

*Corresponding author. Dipartimento di Fisica, INFN - Sezione di Milano, Piazza della Scienza, 3, 20126 Milano, Italy.
E-mail address: Stefano.Pirro@mib.infn.it (S. Pirro).

0168-9002/$ - see front matter © 2005 Elsevier B.V. All rights reserved.
doi:10.1016/j.nima.2005.07.060

ing the crystal mass by a factor 1.65 and reducing the surface-to-volume ratio to 83% of the previous value. The experiment was carried out deep underground, in the Gran Sasso National Laboratories, using two almost identical bolometers inside an Oxford 200 dilution refrigerator that can reach 7 mK.

2. Experimental setup

Both bolometers have, as absorber, a $6 \times 6 \times 6\,cm^3$ TeO_2 crystal, with a heat capacity of $2.33 \times 10^{-9}\,J/K$ at 8.5 mK, as can be calculated assuming a Debye law with $\Theta_D = 232\,K$ [2]. The temperature sensors (for redundancy we decided to glue two of them on each crystal) are $3 \times 3 \times 1\,mm^3$ Neutron Transmutation Doped Ge thermistors, series #31 [3]. They are thermally coupled to the absorber with 9 spots of epoxy glue of ~0.6 mm diameter and ~50 μm thickness. In order to correct for thermal instabilities [4], a ~50 kΩ resistor, realized with a heavily doped meander on a $2.5 \times 2.5 \times 0.5\,mm^3$ silicon chip, is attached to each crystal with one single spot of epoxy glue and is used as a heater. The crystal itself is fastened to a Cu frame by means of 8 S-shaped PTFE supports that hold it in each corner of two opposite faces (see Fig. 1). This setup was modified with respect to that of CUORICINO in order to simplify the assembling procedure and to reduce the number of screws needed. The two independent bolometers are assembled one on top of the other and covered with Cu plates, to form a single box, which is then fastened to the dilution unit of the cryostat through a two-stage damping system, as shown in Fig. 1.

In fact, one of the main sources of noise for bolometers originates [5] from the vibration of the overall cryogenic setup, since the friction between absorber and supports determines sudden heat spots or unwanted temperature fluctuations. The large spread of harmonic frequencies which are involved in the phenomenon implies a noise spectrum that has a $1/f$ roll-off, and is therefore particularly annoying for bolometers, which have very low characteristic frequencies. That is why the damping system to mechanically decouple the

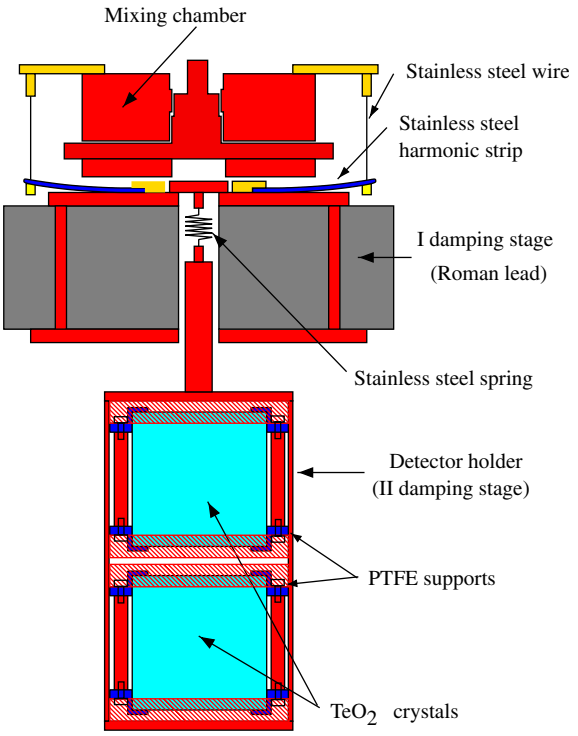

Fig. 1. The two-stage damping system adopted and the two bolometers.

detectors from the cryogenic setup is so important. In this case, the first stage consists of 14 kg Pb disk, with a diameter of 17 cm and a height of 5.5 cm, framed inside a Cu structure. It is mechanically anchored to the cryostat by means of three 4 cm long stainless steel wires, that are connected to the lead through three harmonic stainless steel strips. These strips can slightly bend, resulting in a longitudinal intrinsic oscillation frequency of ~12 Hz. The choice of the lead was driven also by radioactivity reasons, since a 5.5 cm thickness of ancient roman lead [6], that is free of ^{210}Pb (a natural radioactive isotope of Pb), acts as a good radioactive shield against the entire dilution unit components. The second damping stage is realized hanging the detector box from the Cu frame of the lead, through a stainless steel spring and a copper bar. The longitudinal intrinsic oscillation frequency of this second stage is ~5 Hz. The thermal link between the detectors and the cryostat is ensured by two Cu (99.999%) thin

strips of 50 μm thickness linking the Mixing Chamber (MC) to the first stage, and by a second pair of strips linking the first stage to the detector box. The electric contacts for both thermistors and heater are obtained using 50 μm diameter gold wires, ball-bonded on the chips and crimped into very fine Cu tubes, acting as male pins that can be connected to Cu female pins, which are glued onto the frame. From the pins to the MC we used 60 μm diameter constantan wires, in twisted pairs, while 100 μm diameter NbTi wires were used from the MC to room temperature, and in this case the twisted pairs are also shielded by a CuNi wire netting. Two different front-end systems were used. For one of the four thermistors we chose one of the channels available in the cold buffer stage that is thermally anchored at 4.2 K plate, inside the cryostat, while for the other three thermistors a room temperature 12-channel front-end was adopted [7]. The cold buffer stage consists of 12 independent differential channels, composed of 12 pairs of silicon JFET transistors in source follower configuration and 12 pairs of load resistors ($27+27\,G\Omega$) for thermistor biasing. The operating temperature of about 110 K for this stage is achieved by thermally decoupling the two printed circuit boards, each of them housing six channels, from the box in which they are enclosed by means of nylon wires. The thermal impedance thus achieved guarantees the correct temperature to the FETs when they are working, and therefore dissipating. In order to avoid any possible irradiation from the circuit boards, the box is gold plated and is as much as possible hermetic to IR rays. The room temperature front-end and the second stage of amplification are located on the top of the cryostat. The cryostat is shielded against natural radioactivity with an internal layer of copper and an external layer of lead; their minimum thickness are 5 and 10 cm, respectively. In order to eliminate the electromagnetic interference all the setup is enclosed in a Faraday cage. After the second stage, and close to the acquisition system, there is an antialiasing filter (a six pole roll-off active Bessel filter) and a programmable analog triggering and shaping circuit [9]. A small Faraday cage encloses this last stage of amplification. The signals were acquired by a 16 bit ADC embedded in a VXI acquisition system and the data analysis was completely performed off-line.

3. Detector performances

During the entire run, that lasted ~12 days, we observed the crystal holder cooling down following an exponential law. This behavior probably originated from the slow ortho–para conversion of the molecular hydrogen trapped in the copper elements of the detector holder [10]. This effect is a common problem that arises in cryogenics when a mechanical decoupling from the cryostat (which acts also as a thermal decoupling) is introduced. A compromise between the best thermal conductance and the minimum mechanical coupling must be found. This was achieved using the Cu stripes [11] described before between MC and first stage and between the latter and the detector holder. In our case the smallest conductance was between the MC and the first stage, and was measured to be $(2.8 \pm 1.2)\ 10^{-5}\,W/K$ at 8 mK.

The base temperature T_B on the detector holder, reached after 6 days, was ~7.3 mK. We measured the performances of the two detectors at two different holder temperatures: $T_B = 7.3$ and $T_B = 8.8$ mK. The corresponding main properties of the two bolometers (L1 and L2), as read by the two thermistors (#1 and #2), are summarized in Table 1. The thermistor L2#2 was the only one acquired through the cold buffer stage. The energy calibration was performed using a ^{232}Th γ-ray source placed outside the cryostat. The energy resolutions FWHM obtained with the two detectors are summarized in Table 2.

Thermistors mounted on the same crystal showed only slight differences (⩽20%) in energy

Table 1
Main properties of the detectors at two different holder working temperatures $T_{base} = 7.3$ mK ($T_{base} = 8.8$ mK)

	*L*1#1	*L*1#2	*L*2#1	*L*2#2
R (MΩ)	244 (95)	163 (41)	272 (107)	142 (83)
Signal (μV/MeV)	200 (104)	109 (44)	265 (148)	136 (62)
T^{rise} 10–90% (ms)	86 (75)	90 (74)	82 (68)	74 (65)
T^{decay} 90–10% (ms)	170 (194)	244 (275)	150 (168)	234 (249)

Table 2
FWHM resolution (keV) obtained with the two bolometers. The baseline widths, after optimum filtering, are shown in the last column

	583 keV	911 keV	2615 keV	O.F. keV
L1#1	3.3 ± 0.3	3.9 ± 0.4	3.6 ± 0.6	2.4
L2#2	3.4 ± 0.3	3.5 ± 0.4	4.2 ± 0.6	2.5

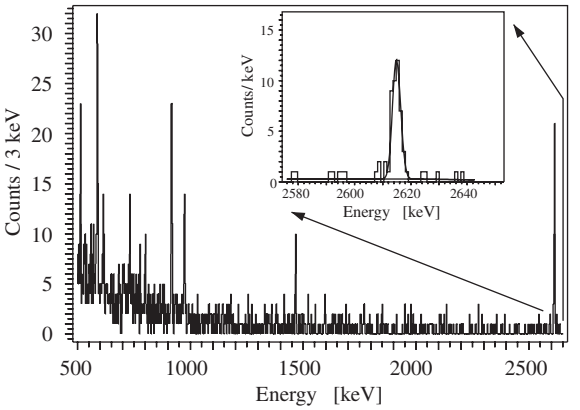

Fig. 2. Calibration spectrum in the γ-ray energy region obtained with one detector exposed for 25 h to a ^{232}Th source. The peak at 2615 keV of ^{208}Tl, magnified in the inset, shows a FWHM resolution of 3.6 keV.

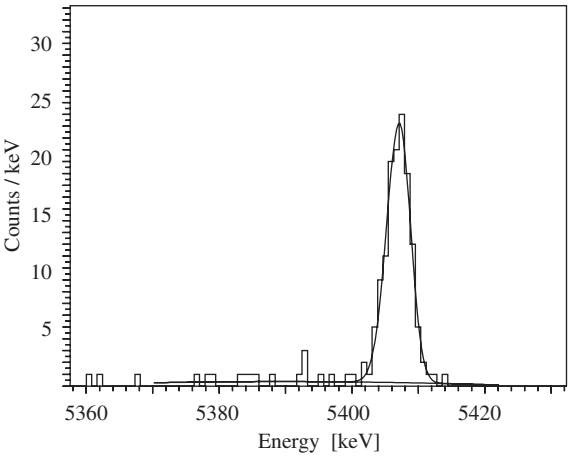

Fig. 3. The α peak of ^{210}Po at 5407 keV.

Table 3
Deviation from the linearity of the detectors at the holder working temperature of $T_{base} = 7.3$ mK ($T_{base} = 8.8$ mK) normalized to the 583 keV γ-line of ^{208}Tl

	*L*1#1	*L*1#2	*L*2#1	*L*2#2
ΔL (%) at 911 keV	0.2 (0.5)	0.1 (0.1)	0.3 (0.4)	0.2 (0.2)
ΔL (%) at 1461 keV	0.5 (1.0)	0.4 (0.8)	0.9 (1.0)	0.4 (0.3)
ΔL (%) at 2615 keV	1.0 (2.2)	0.5 (1.5)	2.0 (2.2)	0.7 (0.6)
ΔL (%) at 5407 keV	1.5 (3.8)	0.4 (2.3)	3.6 (3.9)	0.6 (0.6)

resolutions, probably due to the different microphonic noise coming from the different read-out wires, while the results obtained with the same thermistor at the two T_B were equal within the statistical error. The energy dependence of the resolution is very loose, as it is expected for real calorimeters. The calibration spectrum obtained with the L1#1 detector is shown in Fig. 2.

A very good result was obtained for the α line at 5407 keV due to the internal contamination of ^{210}Po, a common impurity in Te-based materials [12]. We obtained 4.3 ± 0.4 keV with L2 (see Fig. 3) and 5.0 ± 0.5 keV with L1.

These results were obtained without any temperature stabilization of the detector holder, which was slowly cooling down during data taking. This probably caused a slight asymmetry on the full energy peaks, that smeared the energy resolution.

If one tries to evaluate the deviation from linearity of the detectors, expressed as $\Delta L\% = (E^{\text{expected}} - E^{\text{measured}})/E^{\text{expected}}$, where E^{expected} is obtained assuming a linear response of the detector calculated from the lowest calibration line (583 keV) with no offset, an evident dependence from energy shows up, as can be seen in Table 3.

This can be explained by the changes of the thermal parameters of the detectors during the evolution of the signal: the temperature increase due to an energy release in the absorber is small, but finite, with respect to the working temperature. This causes a nonlinear energy response of the detector that can be well described by a simple quadratic form, $E = ax + bx^2$, where x represents the signal in mV. On the contrary, differences within the same crystal and also between two working temperatures can be ascribed to the

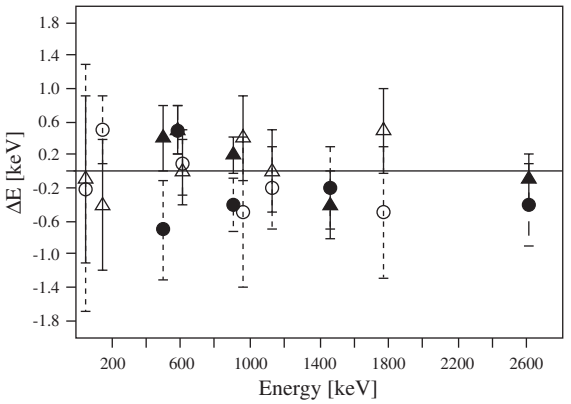

Fig. 4. Deviation between the reconstructed energy and the nominal values for L1#1 (circle) and L2#2 (triangles). The filled markers represent the γ lines used for the linearization fit.

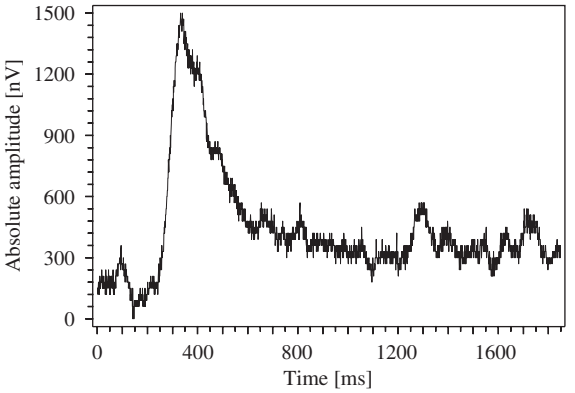

Fig. 5. Typical low energy pulse of L2#2 detector without amplification, corresponding to a deposited energy of 18 keV.

different working points of the thermistors, chosen in order to maximize the S/N ratio.

The linearization fit was calculated including only the more intense lines of the calibration spectrum: 511, 583, 911, 1461, and 2615 keV γ-lines. The corresponding energy of all the peaks present in the spectrum was then evaluated. The deviation between the reconstructed energy and the nominal value of each identified peak is shown in Fig. 4. As it can be seen, the energy reconstruction in the γ region is better than $\simeq 0.6$ keV, showing that the nonlinearity of the detector is well under control.

In many rare events searches, low threshold is essential. Therefore, to evaluate it, the low energy region of detector L2#2 background spectrum was studied. This channel, being the only one read through the cold buffer stage at 4.2 K, showed in fact a less pronounced microphonic noise, which can worsen the threshold level. Using a pulse shape analysis [13], we were able to set the threshold at 12 keV. A typical low-energy pulse from L2#2 detector is shown in Fig. 5.

4. Conclusions

It is the first time that two bolometers heavier than 1 kg show energy resolutions similar to those obtained with Ge diodes. In the Neutrinoless Double Beta Decay region for ^{130}Te (2528.8 keV) the obtained energy resolution is better than the mean energy resolution of the CUORICINO experiment, which is 8 keV. This was achieved thanks to the improved holder design and to the two-stage damping system that minimize the noise induced by the vibrations of the cryogenic apparatus. Thresholds could be certainly improved with less microphonic read-out wires, but this was not our main goal, at least during this test.

Acknowledgements

The results reported here have been obtained in the framework of the R&D program aiming at the optimization of performances of massive thermal detectors in view of the preparation for the experiment CUORE [14] and have been partially supported by the Commission of European Communities under contract HPRN-CT-2002-00322.

Thanks are due to R. Cereseto, A. De Lucia, R. Gaigher, G. Galotta, M. Perego, B. Romualdi, and especially to S. Parmeggiano and A. Rotilio for continuous and constructive help in various stages of this experiment.

References

[1] C. Arnaboldi, et al., Phys. Lett. B 584 (2004) 260
C. Arnaboldi, et al., A new limit on the neutrinoless $\beta\beta$ decay of ^{130}Te, Available from: arXiv:hep-ex/0501034.

[2] M. Barucci, et al., J. Low Temp. Phys. 123 (2001) 303.
[3] E.E. Haller, Infrared Phys. Technol. 35 (1994) 127.
[4] A. Alessandrello, et al., Nucl. Instr. and Meth. A 412 (1998) 454.
[5] S. Pirro, et al., Nucl. Instr. and Meth. A 444 (2000) 331.
[6] A. Alessandrello, et al., Nucl. Instr. and Meth. B 142 (1998) 163.
[7] C. Arnaboldi, et al., Nucl. Instr. and Meth. A 520 (2004) 578.
[9] C. Arnaboldi, et al., IEEE Trans. Nucl. Sci. NS-49 (2002) 2440.
[10] F. Pobell, Matter and Methods at Low Temperatures, Springer, Berlin, 1996 ISBN 3-540-5872-9.
[11] L. Risegari, et al., Cryogenics 44 (2004) 167.
[12] A. Alessandrello, et al., Phys. Lett. B 433 (1998) 156.
[13] S. Pirro, et al., Dark matter results in the MI-BETA experiment, in: D.B. Cline (Ed.), Sources and Detection of Dark Matter and Dark Energy in the Universe, Springer, Berlin, 2001 ISBN 3-540-41216-6.
[14] The CUORE Collaboration, Nucl. Instr. and Meth. A 518 (2004) 775.